# BONDING CFRP-METAL STRUCTURES IN VEHICLES

*O. Hahn*, T. Fuhrmann***

* Laboratory for joining technologies and materials science (LWF), Paderborn University, Germany

** LWF Transfer GmbH & Co. KG, Paderborn, Germany

## 1. Abstract

As weight reduction is required for ecological aspects and in certain areas of the vehicle for dynamic handling requirements, and besides this metallic materials cannot be extensively substituted within the short-term, structurally bonding metallic materials with CFRP is necessary. Cathodic dip painting (CDP), which precedes the bonding process, is able to offer good protection in order to combat sub-surface corrosion (bondline corrosion), which is also familiar from bonded metal joints. If the CFRP structural part has to be painted together with the entire body-in-white, the CFRP component, and therefore the joining process, may be integrated into the production sequence directly downstream of CDP. If joint painting is not necessary, the joining process may be carried out at the beginning of assembly directly following paint drying. High thermomechanical stress in the production process can therefore be avoided and the $\Delta\alpha$ problem is reduced to the vehicle's operating temperature range.

The paper shows the characteristic properties of different adhesive systems, e.g. two-component epoxy, polyurethane or methacrylate, in bonded CFRP-metal joints based on quasi-static test results. Especially the requirements on withstanding thermomechanical stresses in production and vehicle's operating temperature range are shown and evaluated by tests at different temperatures.

The results shown in this article are developed in a cooperation project of Volkswagen AG Wolfsburg, LWF Transfer GmbH & Co. KG and LWF, Paderborn University, Germany.

## 2. Introduction

Increasing safety and comfort demands which are being made on passenger cars and the reduction of fuel consumption are constantly presenting automobile manufacturers with new challenges. The increase in weight caused, e.g. by additional equipment, acoustic measures for reducing noise emission or additional passive safety equipment must therefore be compensated by increasing efforts to implement lightweight design measures throughout the entire vehicle.

In addition to appropriate design measures, the choice of material is vitally important in increasing the extent of lightweight design implemented in the vehicle structure. Materials whose specific (weight-related) stiffness and strengths are higher than those of materials that are conventionally used are of particular interest in this case. In this regard, focus must be placed on endless fibre-reinforced plastics (FRP). For example, the employment of carbon fibre-reinforced plastics (CFRP) may be used to achieve weight reductions of more than 50% in comparison with steel designs and more than 20% in comparison with aluminum designs [1].

As weight reduction is preferable in certain areas of the vehicle due to dynamic handling requirements and, beside this, metallic materials cannot be extensively substituted within the short-term, the necessity of structurally joining metallic materials with CFRP arises.

Problems such as e.g. material thermal expansion differences ($\Delta\alpha$ problem), the provision of suitable surface characteristics for bonding CFRP or CFRP`s anisotropic deformation behavior and strength characteristics additionally arise. When manufacturing CFC metal joints, each electrically conductive connecting element (e.g. rivet) represents a potential source of electrochemical corrosion as a result of the great difference in electrochemical potential. Under this aspect, an elementally bonded CFRP-metal joint would be optimal, as an electrically conductive connection between the carbon fibres and the metal is prevented via the adhesive layer. Cathodic dip painting (CDP) which precedes the bonding process is able to offer good protection in order to combat sub-surface corrosion (bondline corrosion), which is familiar from bonded metal joints.

For CDP drying purposes, the body-in-white passes through a drying furnace, in which temperatures of up to 190°C may occur. Even if this is unproblematic for the temperature resistance of the CFRP structural part on selection of a suitable matrix system, expansion differences of the materials may cause critical deformation or even severe damage to the structure. Following CDP drying, the process temperatures in the paint drying area, at 140°C to 160°C, are already significantly lower, as a result of which mechanical stress in the structure is reduced. If the CFRP structural part has to be painted together with the entire body-in-white, the CFRP component, and therefore the joining process may be integrated into the production sequence directly downstream of CDP. If joint painting is not necessary, the joining process may be carried out at the beginning of assembly directly following paint drying. High thermomechanical stress in the production process can therefore be avoided and the $\Delta\alpha$ problem is reduced to the vehicle's operating temperature range.

For evaluating different adhesives for structural bonds between Cathodic dip painted Aluminum and CFRP the mechanical properties (Young’s modulus) of the adhesives and the lap shear strength of the bonds depending on temperatures in production process and vehicle’s operating temperature range are studied in this article. Furthermore some relaxation tests of the bonds at paint drying temperatures are shown. Failure surfaces are shown and partially analyzed by Raster Electron Microscopy. In order to minimize failures in deformation measurement of the specimens (e.g. caused by tensile test machine rigidity) all tests are done with a special extensometer which was applied (chapter 2).

The results shown in this article are developed in a cooperation project of Volkswagen AG Wolfsburg, LWF Transfer GmbH & Co. KG and LWF, Paderborn University, Germany.

## 2. Materials, Specimen Geometry and Testing Procedures

### Adherend Materials

Single lap shear specimens were made of carbon fibre epoxy laminates manufactured by Resin Transfer Moulding (RTM) and aluminum sheets, which were Cathodic Dip Painted. A biaxial non-crimp fabric was used to manufacture the RTM Plates with the stacking sequence of $[0°/90°/+45°/-45°/]_s$. With the thickness of 1.8 mm, the fibre volume content is given at approximately 45%. Young's Modulus and tensile strength of fibre tensile failure and transverse tensile failure are given in *Table I*. The aluminum sheets with the thickness of 2.5,mm were heat treated with the Cathodic Dip Paint drying process, so that the given yield and tensile strength were reached.

### Adhesives

Four different adhesive systems were used for the tests:

- 2-component cold curing Methacrylate (MA)
- 2-component cold curing Polyurethane (PU)
- 2-component cold curing Epoxy (EP2)
- 1-component hot curing Epoxy (EP1)

*Table II* shows specification and mechanical properties of the adhesives. All data are given by the technical data sheets of suppliers according to the named norm. Surface preparation was done for all adhesives on both adherends by cleaning with heptane only. Cold-curing adhesives were cured for 7 days at room temperature. The 1-component hot-curing Epoxy was cured for 30 minutes at 160°C.

### Specimen Geometry

*Figure 1* shows the geometry of single lap-shear specimens. The overlap length was chosen at 14 mm. The thickness of adhesive layer was 1 mm and joint width was 45 mm. For reaching a constant spew fillet angled normal to the adherend surface, the protruding adhesive at the end of overlap length was striped off after assembling the adherends. In order to clamp the specimen in tapered clamping jaws, which were used for the test in climatic chamber, doublers were applied at the ends of the specimen. Furthermore, a small doubler was applied in a distance of 2 mm from the end of overlap length on the aluminum adherend to fix the extensometer for displacement measurement.

### Dynamic Mechanical Analysis (DMA)

Dynamic mechanical analysis was performed in a dual-cantilever-bending load case with small amplitudes of 30 µm at a frequency of 1 Hz. The free bending length was 5 mm each side. *Figure 2* shows the geometry of dual-cantilever bending test. The temperature range was chosen from -50°C to +196°C, performed with a heating rate of 2°C/min. For calculation of the storage modulus, the standard beam theory assumptions were applied.

### Single Lap-Shear Test

Single lap-shear tests were performed in displacement control of the clamping jaws at a rate of 2 mm/min until failure of the joint. The free clamping length was selected at 125 mm. In order to minimize failures in deformation measurement of the specimens (e.g. caused by tensile test machine rigidity), all tests were done with a special extensometer, which was applied during the test. *Figure 3* shows schematically the application of extensometer in undeformed and deformed shape of the specimen. One test series consists of five lap shear tests. In the following diagrams showing the lap shear strength or the stress-displacement curve, the average value of the five tests or a representative curve of the series is presented.

### Relaxation Test

Relaxation test were done at 160°C. Based on a single lap-shear test series at this temperature, the average displacement at failure was determined. During the relaxation test a defined percentage of this value was adjusted in displacement control of the clamping jaws. Starting from here, the displacement value, measured by applied extensometer, was kept constant and the force value was recorded. The time period of recording the force was assimilated to a paint drying process. Displayed force-time curves show a representative curve of the series. In this article, two different degrees of displacement – 25% and 75% of displacement at failure – are presented.

After having passed the relaxation test, a single lap-shear test at room temperature was carried out with the specimens to investigate a mechanical damage represented in a lower lap shear strength.

## 3. Results and Discussion

### Dynamic Mechanical Analysis

*Figure 4* shows the storage modulus of the adhesives depending on the temperature. The cold-curing Polyurethane and Epoxy adhesives have the lowest glass-transition temperature, lying in the working temperature range of the vehicle's body structure (-30°C to –90°C). Higher glass-transition temperatures are offered by the hot-curing Epoxy and the cold-curing Methacrylate adhesive. Whilst the 1-k EP, the 2-k EP and the 2-k MA are characterized by nearly the same modulus at the energy-elastic state (high modulus level), there are differences in modulus at the entropy-elastic state (low modulus state), so that the 2-k EP at a temperature of more than 150°C has the highest modulus. Compared to these adhesives, the 2-k PU shows a significantly different level of modulus at low and high temperatures. On both ends of the illustrated temperature scale, the modulus of the 2-k PU is more than three times as high as that of the other shown adhesives.

The change of the adhesive modulus in an adhesive joint, e.g. at glass-transition temperature is theoretically (linear-elastic analysis) followed by a significant change in deformation behavior of the joint. Between the changing modulus, the strength of the adhesives depend on the temperature, too.

In order to find out how these effects result in the strength of bonded joints, lap-shear tests were carried out at –30°C, room temperature (RT), 90°C and 160°C. In the following the load-displacement curves, the lap shear strength and the failure surfaces of the joints are presented and analyzed for the different adhesives.

## Quasi-Static Load-Displacement Behavior at Room Temperature (RT)

Figure 5 illustrates the characteristic stress-displacement curves of the different adhesives at RT. The average shear stress is calculated by dividing the load by the overlap area of the joint. The displacement is measured by the extensometer.

The curves show the different deformation behavior between the two EP and the MA or the PU adhesive. Whilst the EP Systems have an ultimate strain of approximately 8-10 percent resulting in low deformations at failure of the joint, the PU and the MA offer ultimate strains of more than 70%, followed by high deformations at failure of the bonded joints. All bonded joints fail at 18 to 21 MPa average shear stress (see *Figure 7*). In the quasi-linear-elastic part of the curves, the differences in modulus presented are very good. A lower stiffness of the PU joint was observed compared to the other systems, caused by the lower modulus (in between glass-transition temperature range) of the PU. Linear-elastic behavior is noticed only up to 30% of failure load for this adhesive. For the MA and the two EP systems, up to 70% a linear-elastic behavior is shown. The MA combines high elastic deformations and stiffness like the EP systems with high deformation to failure like the PU system.

Considering the failure surfaces in *Figure 6,* a cohesive failure is observed for the PU system. The MA joint shows a surface-near cohesive failure on CFRP with small areas of breaked-away EP-Matrix situated there, where the sticking yarn is near the surface. Both EP joints show a breakaway of the CDP, combined with a cohesive failure especially at the 2-k EP joint. Total delamination of CFRP was not observed in all the joints.

An explanation for the different deformation behavior between the different adhesives and the resulting failure surfaces is tried in the following sub-chapter supported by a linear-elastic analysis of the joints.

## Linear-Elastic Analysis of Adhesive Stresses at RT

*Figure 7* illustrates a linear-elastic analysis of the stress distribution of a high-modulus 1-k EP joint vs. a low modulus 2-k PU joint at an average shear stress of five Mpa in the tested joint geometry. It is observed that the shear stresses as well as the normal stresses are quite inhomogeneous distributed in the EP joint with high peaks at the ends of overlap length. The shear stress distribution in the PU joint is quite homogeneous whereas the normal stresses increase significantly to the ends of overlap. As the maximum peel stresses $\sigma_Z$ of the 1-k EP at the end of overlap length amount approximately 50% of tensile strength, the 2-k PU peak stresses reach only 27% of the tensile strength given in *table 2*. Increasing the load the increasing shear- an normal peak stresses at the EP joint lead to a break-away of the CDP before the tensile strength of the adhesive is reached. In contrast to that the high deformation performance and the low modulus of the PU remains the stress distribution in the joint more constantly, so that a cohesive failure occurs at the same lap shear strength. As a consequence of this theory an increasing the tensile strength of the PU would perform a higher lap shear strength of the joints.

As mentioned above the strength of the joints in the whole vehicle’s working temperature range and at temperatures in production process are of interest and will therefore be discussed in the following sub-chapter.

### Lap Shear Strength at Different Temperatures

*Figure 8* shows the lap shear strength of the joints at –30°C, RT, +90°C and +160°C. As described the strength at RT is nearly the same for all the adhesives. At a temperature of–30°C, the MA shows the best deformation performance between the adhesives, resulting in the highest lap-shear strength. The EP and PU joints failed at lower loads compared to room temperature. With increasing temperature the failure load of all joints decreases significantly. Highest loads at 90°C would be transferred by the 1-k EP and the MA, corresponding to the decreasing modulus at the glass-transition temperature range of the adhesives (see *Figure 4*). A further increase of testing temperature leads to even smaller lap shear strength values for all the joints at 160°C. The highest failure load at this temperature is shown by the PU, as might be supposed because of the higher modulus at this temperature compared to the other adhesives.

As the application of such high temperatures to the polymer adhesives might cause relaxation effects, some lap shear tests were performed as described in chapter 2.

### Relaxation Tests at 160°C

As *Figure 9* illustrates, two different degrees of deformation were applied to the PU joints. At a degree of 25% of deformation at failure, a slightl decrease of the applied force is observed, reaching a loss of 50% after 1.000 seconds. All specimens tested under this conditions failed at an average shear stress of approximately 20 MPa in the following lap-shear test at room temperature, so there is no change to the specimen's strength that did not pass the relaxation test. The application of 75% of deformation at failure caused two different characteristics in the force-time curves. Some specimens showed a relaxation in force of about 50% during 1000 seconds like the lower deformed specimens. In some tests of the 75% series, an abrupt decrease of the force occurred after a few seconds (*Figure 9*, Specimen No. 4). Afterwards the force decreases very similar to the 25% test series. After finishing the test on these specimens, a local damage of the adhesive layer was visible on one side of the specimen (*Figure 10*). Starting at the end of overlap length near the surface of the CFRP adherend, a shear crack ran through the adhesive layer to the surface of the cathodic dip-painted aluminum adherend. On the other side of the specimen, no crack was visible.

After performing the single lap-shear tests at room temperature with these specimens, the failure surfaces showed what happened. At relaxation, test between 20% and 50% of the overlap area failed. The failure surfaces show a surface near cohesive failure in these areas. During the lap-shear tests at RT, the cohesive failure in the middle of the adhesive layer (similar to the specimens that did not pass the relaxation test) occurred (*Figure 11*). Relating the failure load of these specimens to the cohesive failure area (at RT), the strength of approximately 20 MPa was reached again.

Raster electron microscopy photographs of the surface near the areas of cohesive failure in the PU joints illustrated that a rest of the adhesive was kept on the aluminum or the CFRP surface (*fFgure 12*).

## 4. Conclusions and Future Work

The single lap-shear tests prove that the MA offers in the temperature range from -30°C to 90°C the best compromise in case of rigidity, deformation performance and strength of the bonded joints. Furthermore, the MA performs with the highest glass-transition temperature between the regarded cold-curing adhesives.

The PU adhesive might be able to transfer even higher loads if its tensile strength might be increased together with keeping the modulus constant. Between that, the PU joints show a very small range of linear-elastic behavior.

The effect of the different load-displacement behavior between the different adhesives on the fatigue life of the joints and on the behavior under impact load should be studied in the future. Different constructive factors on the load-displacement behavior, e.g. overlap length, thickness of the adhesive layer and adherends are done in time.

Relaxation tests show that there seems to be a critical deformation border, which should not be exceeded in order to avoid damage to the joint in the manufacturing process. Test series to investigate such effects are running.

The surface near failure of the joints (depending on the test temperature) suppose that the mechanical properties of the adhesive layer is inhomogeneous [NONHOMOGENEOUS?] through the adhesive's layer thickness. In order to simulate the strength of such joints, the possibility to use the force-displacement curve as an input for simulation should be investigated.

## Acknowledgments

This work has been strongly supported by Volkswagen AG, group research. Special thanks are given to all people of the materials department who gave assistance to the project by a lot of critical discussions and helpful tips. I want to thank my mentor Prof. Dr. O. Hahn for giving me the possibility to work on this project. Furthermore, thanks are expressed to all the students and colleagues of LWF Paderborn who have supported the work so far.

## References

[1] Kopp, J.; Friedrich H.; Gänsicke, T. and H. Henkelmann: Faser-Kunststoff-Verbunde (FKV) für Niedrigst-Verbrauchs-Fahrzeuge; DGM conference presentation, July 2003

[2] Hahn, O.; Hennemann, O.-D. and M. Schlimmer: Entwicklung von Berechnungsmethoden für Stahlklebverbindungen (current research project)

[3] Hahn, O.; Hennemann, O.-D. and K. Dilger: Untersuchungen zum Crashverhalten geklebter und hybridgefügter Stahlblechverbindungen, Concluding research project report, P. 477

[4] Ruther, M.; Jost, R.; Freitag, V.; Peitz, V.; Piccolo, S.; Brüdgam, S.; Meschut, G.; Küting, J.; Hahn, O. and R. Timmermann: Fügesystemoptimierung zur Herstellung von Mischbauweisen aus Kombinationen der Werkstoffe Stahl, Aluminium, Magnesium und Kuststoff; Concluding public report on BMBF project 03N3077D1, 187 pages, July 2003

[5] Meschut, G. and T. Gänsicke: Experimentelle und rechnerische Analyse der Klebschichtbeanspruchung in Verbindungen aus thermisch inkompatiblen Werkstoffen; Schweißen und Schneiden 55 (2003) Issue 7, P. 371-383

[6] Hahn, O.: Festigkeitsverhalten und ingenieurmäßige Berechnung von einschnittig überlappten Metallklebverbindungen, Habilitationsschrift Technische Hochschule Aachen, 1975

[7] Maibaum, Dirk: Mechanisches Verhalten von Metallklebverbindungen bei ein- und mehrachsiger Kurz- und insbesondere Langzeitbeanspruchung, Dissertation, Universität Paderborn, LWF, 1990

[8] Hahn, O. und Hüsgen, B.: Erarbeitung von technologischen Grundlagen für das Kleben von Fügeteilen mit unterschiedlichen Ausdehnungskoeffizienten; Forschungsbericht des LWF; Universität Paderborn, 1991

[9] Matthews, F. L. et. al.: Joining fibre-reinforced plastics; Elsevier Applied Science, 1987, ISBN: 1-85166-019-4

## 7. Tables and figures

*Table I: Specification of adherend materials.*

| | Adherend 1: CFRP | Adherend 2: Aluminum AA6016 T6 |
|---|---|---|
| **Thickness** | $t_1$: 1.8 mm | $t_2$: 2.5 mm |
| **Specification / Stacking sequence** | 0°/90°/+45°/-45°/–45°/+45°/90°/0° | AlMg0.4Si1.2 (AA6016) heat treatment status: T6 |
| **Young's modulus** | 45 000 MPa | 70 000 Mpa |
| **Tensile strength** | Transverse tensile failure: 250 MPa<br>Fibre tensile failure: 625 MPa | Yield strength: 210 MPa<br>Tensile strength: 260 MPa |
| **Thermal expansion coefficient** | $\alpha_{CFK}$: approx. $5x10^{-6}$ 1/K | $\alpha_{Al}$: approx. $24x10^{-6}$ 1/K |

*Table II: Specification of adhesive materials.*

| | 2-k Methacrylate (MA) | 2-k Polyurethane (PU) | 2-k Epoxy (EP2) | 1-k Epoxy (EP1) |
|---|---|---|---|---|
| **Tensile strength** | 20 MPa<br>ISO R 527 Type | 15 MPa<br>DIN 53504 | 29 MPa<br>EN ISO 527-1 | 40MPa<br>EN ISO 527-1 |
| **Lap shear strength** | 16 MPa<br>ISO 4587<br>curing: 2 days at 23°C<br>Aluminum L165, sanded | 15 MPa<br>EN 1465<br>adhesive thickness: 1mm | 17,6 MPa<br>EN 1465<br>curing: 2 days at 23°C<br>Aluminum AC120 (AA6016) | 26,9 MPa<br>EN 1465 |
| **Young's modulus** | 1584 MPa<br>calculated from shear-modulus with Poisson's ratio 0,32 | 130 MPa<br>DIN 53504 | 1700 MPa<br>EN ISO 527-1 | 1800 MPa<br>EN ISO 527-1 |
| **Shear modulus** | 600 MPa<br>DIN 53345<br>curing: 7 days at 23°C | 50 MPa<br>DIN 54451 | 643 MPa<br>calculated from Young's-modulus with Poisson's ratio 0,32 | 682 MPPpa<br>calculated from Young's-modulus with Poisson's ratio 0,32 |
| **Elongation at break** | 35-50%<br>ISO R 527 Type | 100%<br>DIN 53504 | 9%<br>EN ISO 527-1 | 14%<br>EN ISO 527-1 |
| **Pot life** | 4-5 min<br>10 g at 25°C | 15-20 min | 60 min | - |
| **Curing** | 7 days at room temperature | 7 days at room temperature | 7 days at room temperature | 30 min at 160°C |

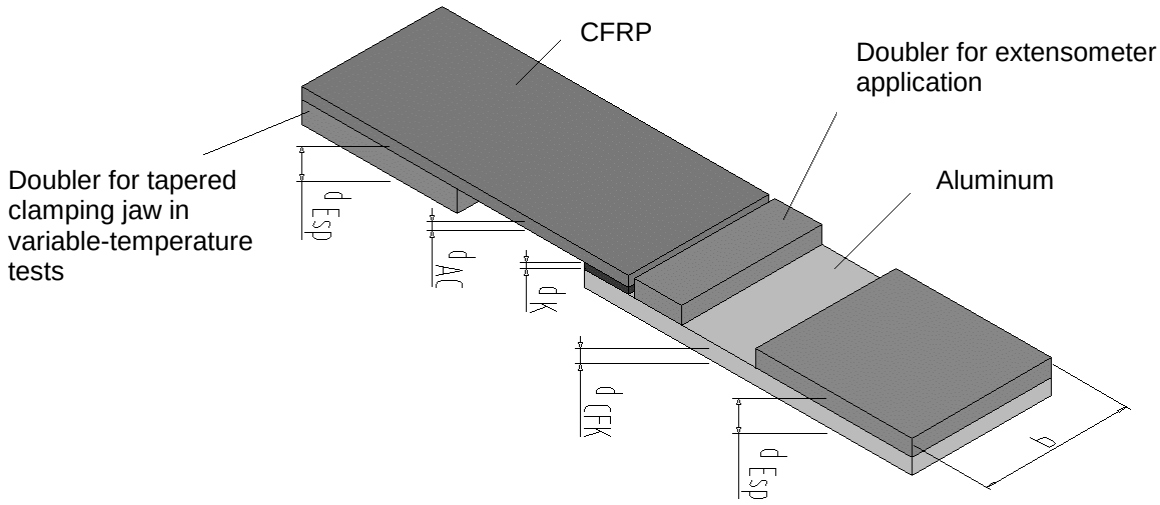


CFRP thickness: $t_1$ = 1,8mm ($[0/90/+45/-45]_s$)
Aluminum thickness: $t_2$ = 2,5mm (Cathodic dip painted)
Adhesive thickness: $d_k$ =1mm
Specimen width: b = 45mm
Clamping length: $L_E$ = 125mm
Overlap length: $L_Ü$ = 14mm

*Figure 1: Geometry of single lap-shear specimens.*

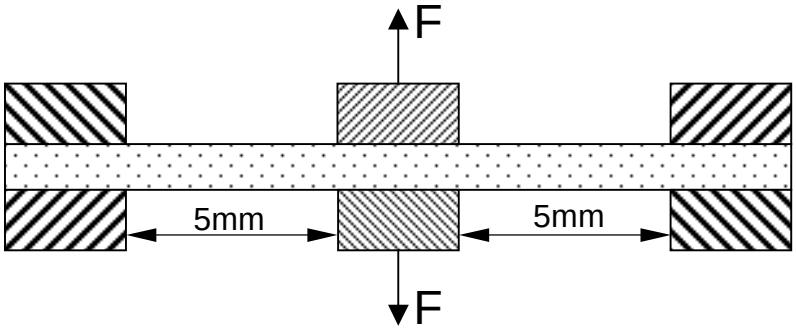


*Figure 2: Geometry of dual-cantilever bending test in Dynamic Mechanical Analysis.*

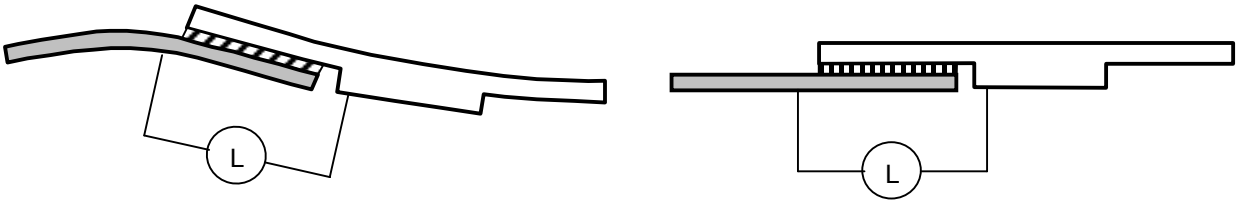


*Figure 3: Application of extensometer on undeformed and deformed specimens.*

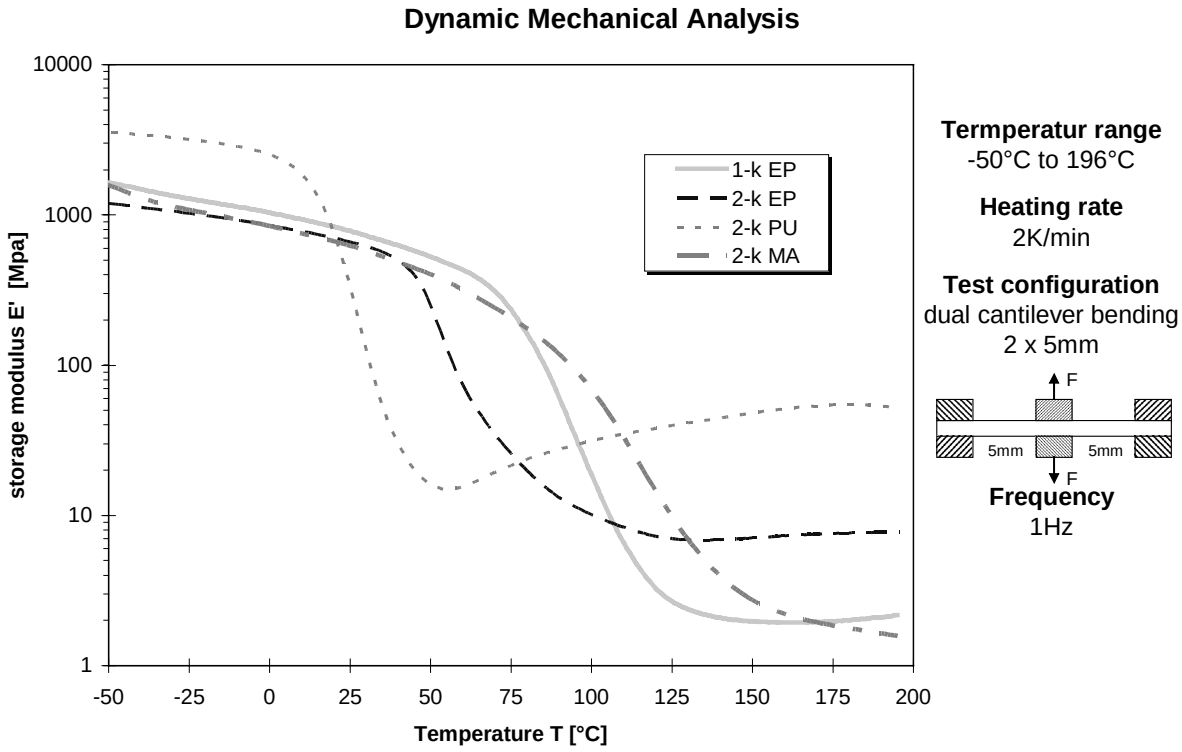


*Figure 4: Storage modulus of adhesives depending on temperature (Dynamic Mechanical Analysis).*

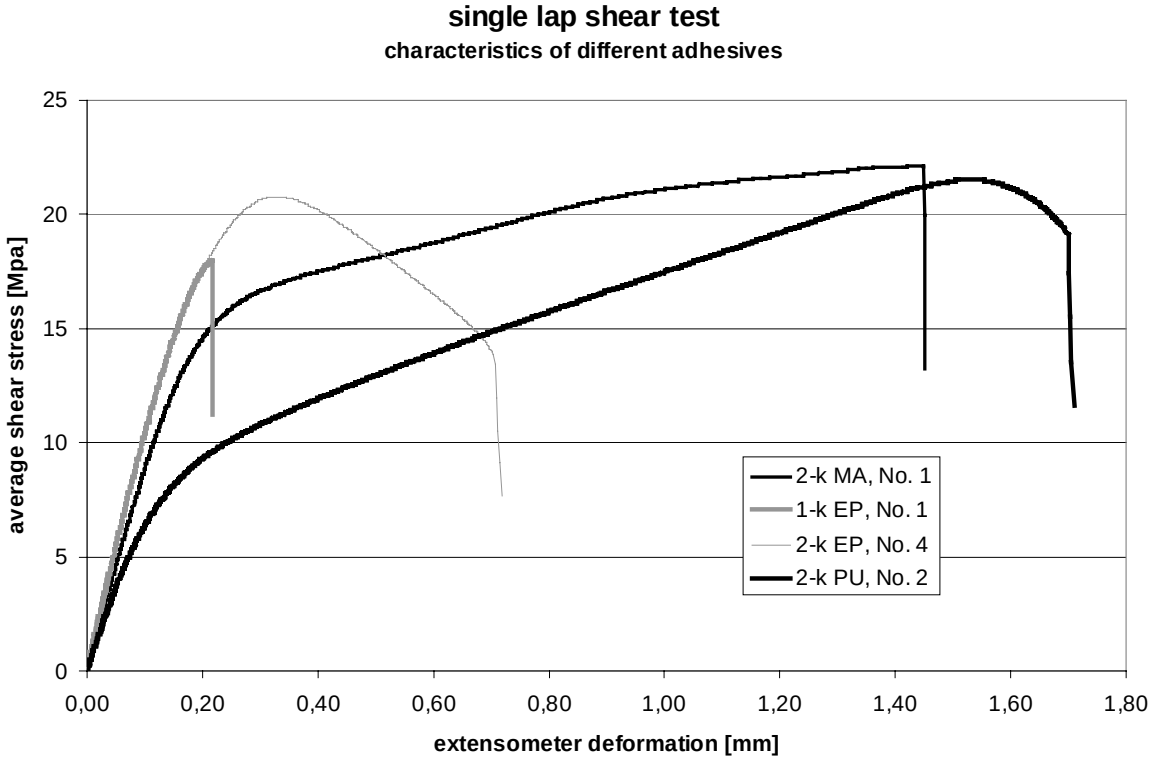


*Figure 5: Characteristic stress-displacement curves of lap-shear specimens at room temperature (RT).*

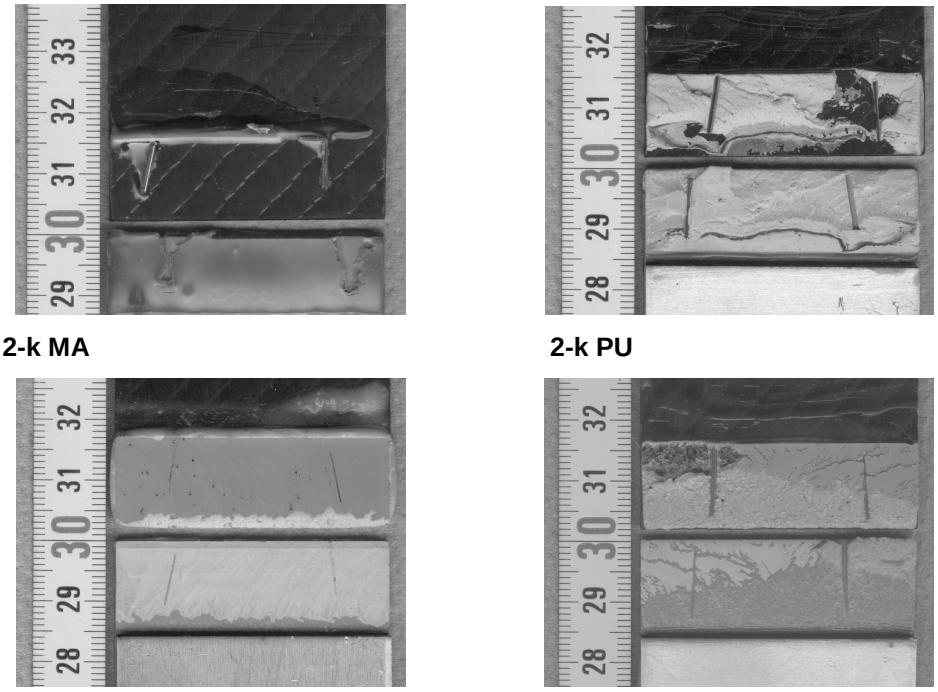


*Figure 6: Failure surfaces of lap-shear specimens tested at room temperature (RT).*

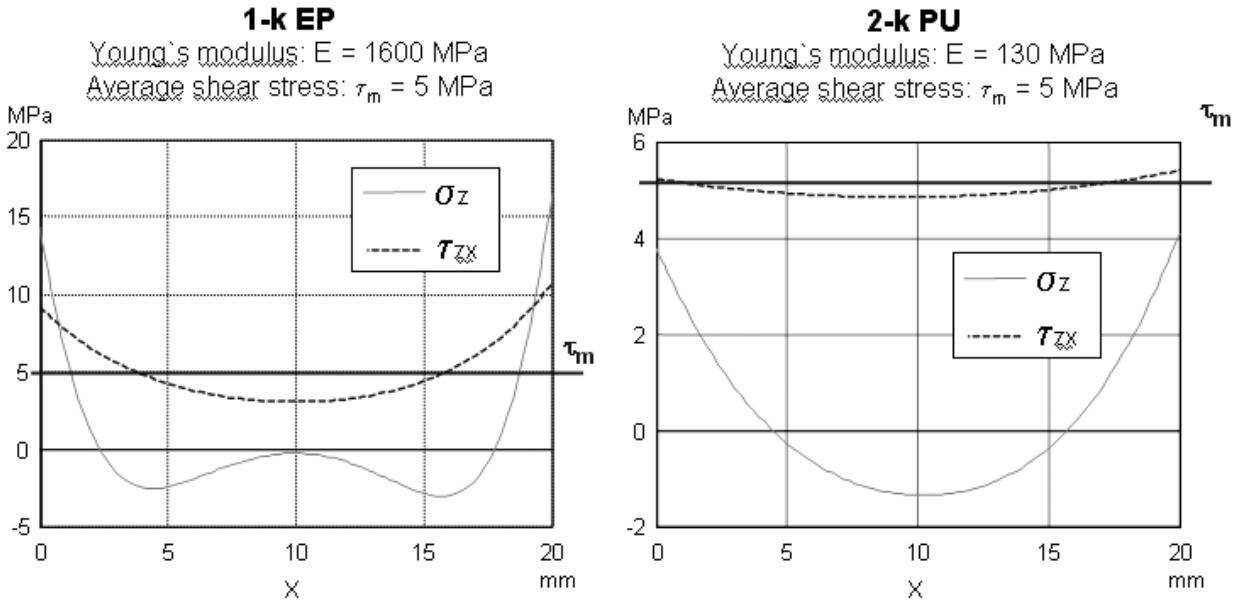


*Figure 7: Normal- and shear-stress distribution of 1-k EP and 2-k PU adhesive (linear-elastic analysis).*

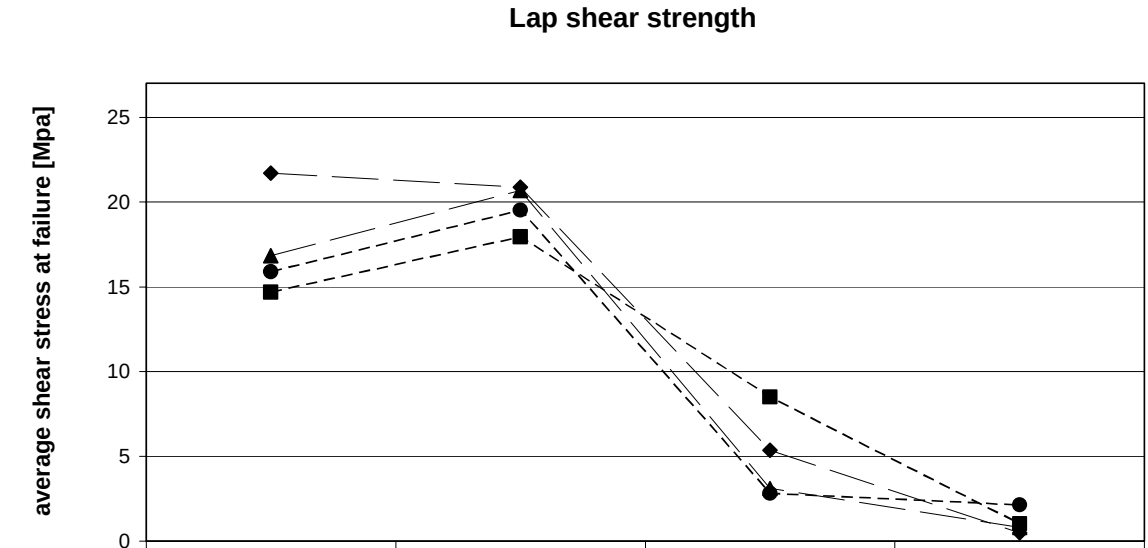


| | -30°C | RT | 90°C | 160°C |
|---|---|---|---|---|
| 2-k MA | 21,70 | 20,88 | 5,36 | 0,49 |
| 2-k PU | 15,89 | 19,53 | 2,82 | 2,13 |
| 2-k EP | 16,83 | 20,69 | 3,10 | 0,81 |
| 1-k EP | 14,68 | 17,94 | 8,51 | 1,01 |

*Figure 8: Lap-shear strength of tested adhesives depending on test temperature (line: "guide to the eye").*

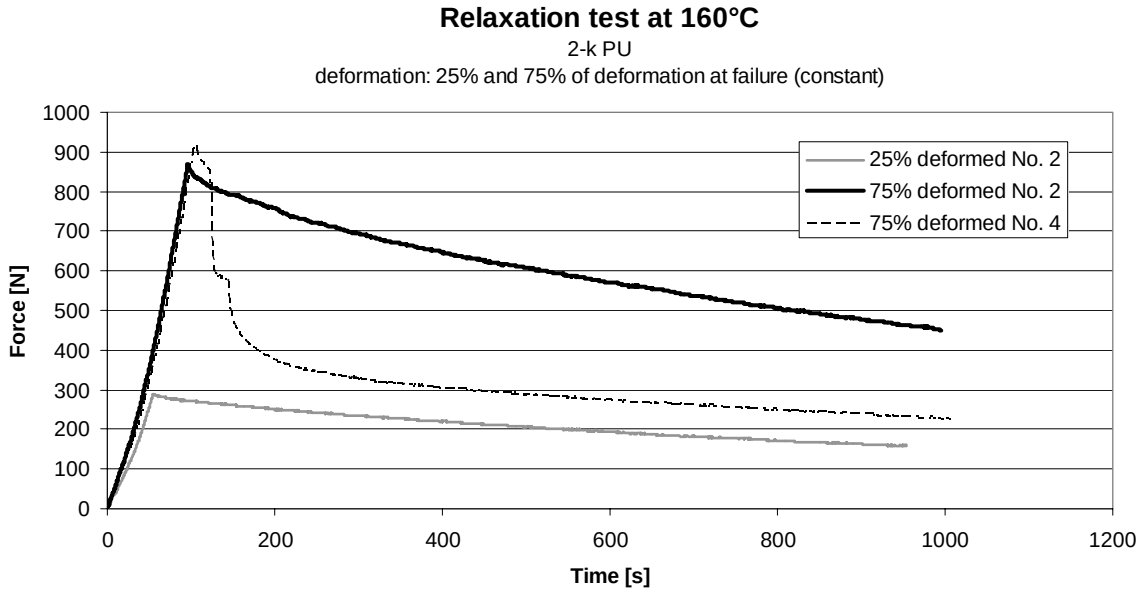


*Figure 9: Force-time curves of the lap-shear specimens tested in relaxation test at 160°C.*

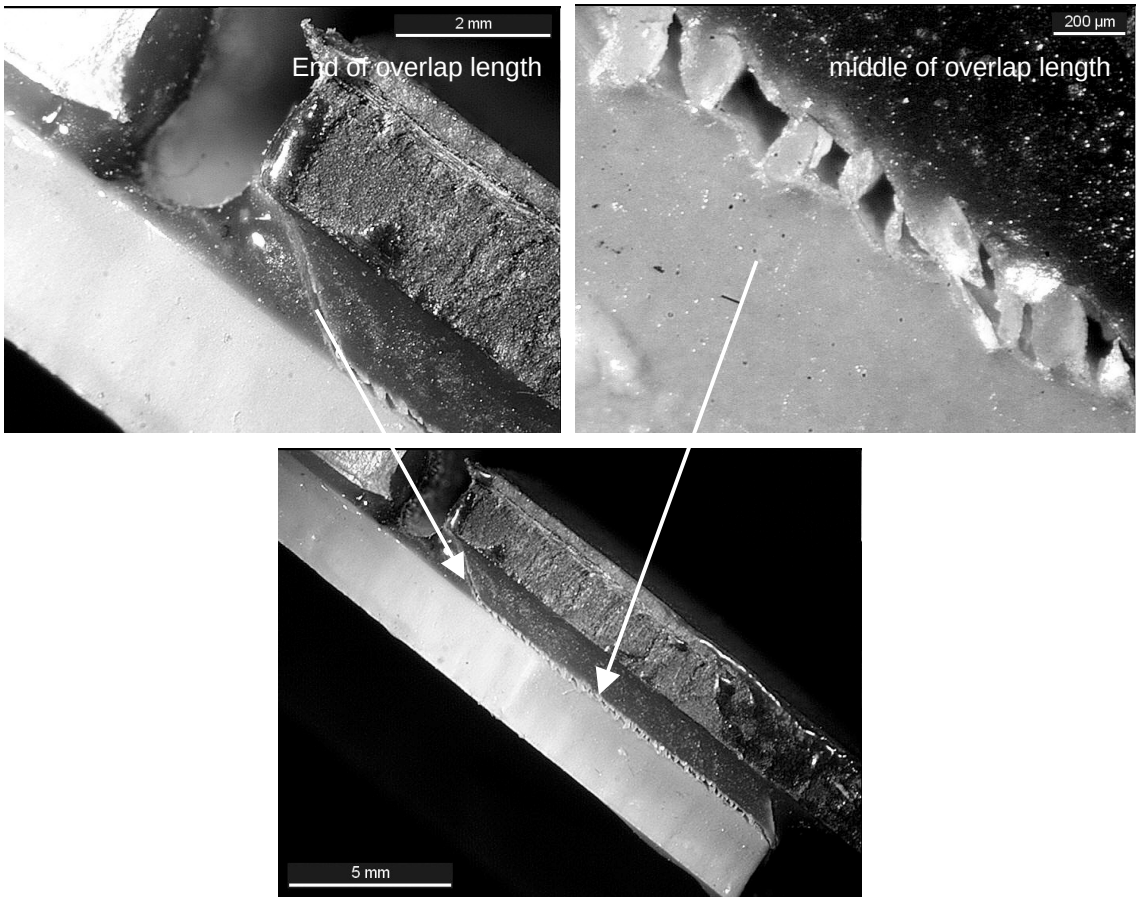


*Figure 10: Photograph of partially damaged adhesive layer (75% relaxation test series).*

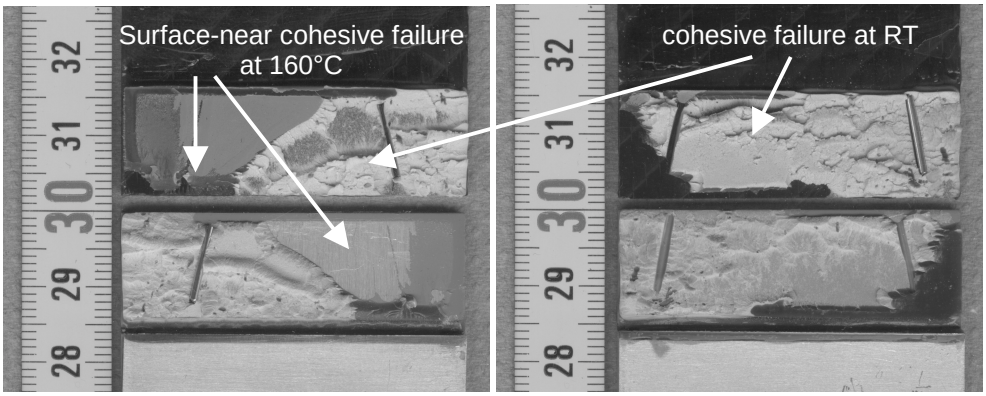


*Figure 11: Failure surfaces of lap-shear specimens tested in relaxation test at 75% of deformation at failure.*

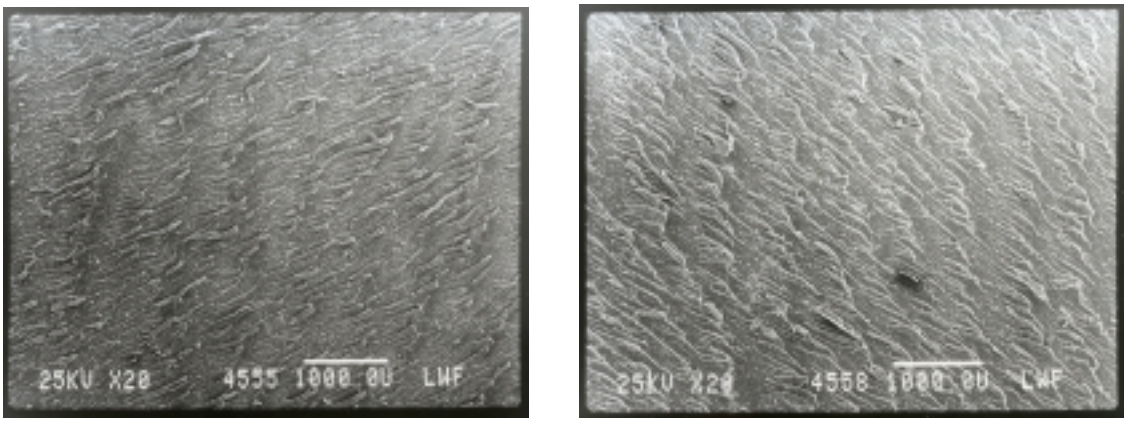


*Figure 12: Raster Electron Microscopy of 160°C (2-k PU) failure surfaces at CFRP (left) and AA6016 (right).*